

Theoretical study of intramultiplet transitions in collisions of atoms in 3P electronic states with structureless targets: $\text{Ca}(^3P) + \text{He}$

Millard H. Alexander, Tadeusz Orlikowski,* and John E. Straub†

Department of Chemistry, University of Maryland, College Park, Maryland 20742

(Received 17 January 1983)

The quantum close-coupling (CC) treatment of collisions of an atom in a 3P electronic state with a structureless target is developed, based on earlier work of Mies [Phys. Rev. A **7**, 942 (1973)], and a j_z -conserving [coupled-states (CS)] simplification presented. There is no direct coupling between the $J=0$ and $J=1$ levels; transitions between these levels will occur only as a result of Coriolis coupling involving the $J=2$ state. Actual CC and CS calculations are reported for collisions of $\text{Ca } 4^3P^o$ with He, based on the potential curves of Malvern [J. Phys. B **11**, 831 (1978)]. In the CC results, of the three independent cross sections, $J=2 \rightarrow 1$ is predicted to be largest, and $J=2 \rightarrow 0$ smallest, over the entire range of collision energies sampled. By contrast, the CS approximation predicts the $1 \rightarrow 0$ transition to be forbidden, and yields only fair accuracy for the CC $2 \rightarrow 1$ and $2 \rightarrow 0$ transitions. The coupling between spin-orbit states is also interpreted within an adiabatic model. A comparison with the experimental results of Yuh and Dagdigian (preceding paper) is made by averaging the CC cross sections over the experimental translational energy distribution. The experimental cross sections for the $2 \rightarrow 1$ and $2 \rightarrow 0$ transitions are 3–4 times larger than the theoretical values, and the $2 \rightarrow 0$ cross section is found experimentally to be ~ 3 times larger than the $1 \rightarrow 0$ cross section, in direct contrast with the theoretical prediction for this ratio.

I. INTRODUCTION

There has been much interest in the past in the theory of fine-structure changing collisions in atomic collisions, in particular collisions of atoms in 2P electronic states with closed shell atoms. Nikitin and collaborators^{1,2} have carried out a continuing series of investigations of these processes, within a semiclassical treatment of the collision dynamics. There have also appeared a number of fully quantum studies,^{3–13} based on formalisms presented first by Reid and Dalgarno^{3,4} and by Mies.⁵ Relatively little attention has been paid to collisions of atoms in 3P states, where three distinct fine-structure-changing transitions will occur, as compared with the unique transition which characterizes the well-studied 2P systems. There have been several studies of 3P systems using semiclassical methods^{14–16} or elastic-scattering models¹⁷; Cohen, Collins, and Lane¹⁸ have determined cross sections for the $\text{Ne}(^3P) + \text{Ne}$ system using an approximate close-coupling treatment; and, recently, Aquilanti and co-workers^{19–21} have discussed quantum decoupling approximations which may be suited to this type of collision. *Ab initio* potential curves for the interaction of noble-gas atoms with alkaline-earth atoms in 3P electronic states have been reported by Malvern²² and by Demetropoulos and Lawley.²³

Motivated by the recent experimental study by Yuh and Dagdigian,²⁴ we have undertaken a companion theoretical investigation of fine-structure changing collisions of alkaline-earth atoms with helium atoms, using a fully quantum description of the collision dynamics. The formalism, presented in the next section, is an extension of the work of Mies.⁵ The Ca-He potential curves of Malvern,²² discussed in Sec. III, were used to describe the interaction. Calculations were carried out within a full close-coupling treatment and within a j_z - (or Ω -) conserving simplification, identical to that described by various authors.^{10,18,20,21,25} Our goal is to explore the range of va-

lidity of this dynamical approximation and to investigate the degree to which accurate quantum-scattering calculations can reproduce the experimental data of Yuh and Dagdigian.²⁴ These calculations are described in Sec. III and the results presented and discussed in Sec. IV. These results are interpreted in terms of an adiabatic formulation^{1,14,26} in Sec. V. The comparison between our calculations and the experimental intramultiplet cross sections reported in the preceding article²⁴ is made in Sec. VI. A brief conclusion follows.

II. FORMULATION OF THE DYNAMICS

As stated in the Introduction, we follow the approach presented by Mies⁵ for collisions of $\text{F}(^2P)$ with H^+ . Asymptotically, the wave function for the $M(^3P) + N(^1S)$ system will be written as $|N\rangle |\Lambda \Sigma n L S\rangle$, where $|N\rangle$ denotes the wave function of the noble gas and the wave function of the metal atom is specified by the orbital and spin angular momenta (L and S), their projections along the M - N axis (Λ and Σ), and an index n which denotes the electronic state of the metal atom. The total electronic Hamiltonian is given by

$$H_{MN}(\vec{r}_M, \vec{r}_N; R) = H_{MN}^0(\vec{r}_M, \vec{r}_N; R) + V_{LS}, \quad (1)$$

where

$$H_{MN}^0(\vec{r}_M, \vec{r}_N; R) = H_M(\vec{r}_M) + H_N(\vec{r}_N) + V_{MN}(\vec{r}_M, \vec{r}_N; R). \quad (2)$$

Here H_M and H_N denote the electronic Hamiltonians of the M and N atoms; V_{LS} is the spin-orbit operator; the coordinates of the electrons are denoted by \vec{r}_M and \vec{r}_N ; and V_{MN} denotes the electrostatic interaction between the two atoms, which depends parametrically on R , the M - N distance. We assume that V_{MN} vanishes as $R \rightarrow \infty$.

Within the Born-Oppenheimer approximation the elec-

tronic eigenfunctions of a diatomic system are traditionally designated by the quantum numbers Λ, Σ, L, S . We have

$$H_{MN}^0 |R, \Lambda \Sigma nLS\rangle = W_{\Lambda \Sigma nLS}(R) |R, \Lambda \Sigma nLS\rangle, \quad (3)$$

where, as before, the index n will designate the particular electronic state of the two-atom system. The eigenfunctions $|R, \Lambda \Sigma nLS\rangle$ are the *adiabatic* electronic states of the molecular system, as would be given by an *ab initio* calculation, and behave asymptotically as

$$\lim_{R \rightarrow \infty} |R, \Lambda \Sigma nLS\rangle = |N\rangle | \Lambda \Sigma nLS\rangle. \quad (4)$$

The corresponding relation for the Born-Oppenheimer energies is

$$\lim_{R \rightarrow \infty} W_{\Lambda \Sigma nLS}(R) = E_{nLS} + E_N, \quad (5)$$

where E_{nLS} and E_N denote the electronic energies of the M and N atoms.

The electronic states which correlate asymptotically with atoms in the 3P and 1S states are $^3\Pi$ and $^3\Sigma$. The reflection symmetry of the latter state will be Σ^+ if the atom has an sp configuration (3P_u) and Σ^- if the atom has a p^2 configuration (3P_g).²⁷ The electronic energies are independent of the signs of Λ and Σ , and for simplicity will be denoted as $W_{\Pi}(R)$ and $W_{\Sigma}(R)$. Since the quantum numbers n, L , and S have the same values for both the $^3\Pi$ and $^3\Sigma$ states, these indices will be dropped unless explicitly needed.

Linear combinations of the electronic eigenfunctions can be taken which are eigenfunctions of the total angular momentum $\vec{J} = \vec{L} + \vec{S}$, namely,

$$|R, J\Omega\rangle = \sum_{\Lambda, \Sigma} (L \Lambda \Sigma | LSJ\Omega) |R, \Lambda \Sigma\rangle, \quad (6)$$

where Ω is the projection of \vec{J} along the M - N axis and $(L \Lambda \Sigma | LSJ\Omega)$ is a Clebsch-Gordan coefficient. The matrix elements of the electronic Hamiltonian between these total angular momentum states are given by

$$\begin{aligned} \langle J'\Omega' | H_{MN} | J\Omega\rangle = & \delta_{\Omega\Omega'} \left[\delta_{JJ'} \left[W_{\Pi} + \frac{a(R)}{2} [J(J+1) - L(L+1) - S(S+1)] \right] \right. \\ & \left. + [(2J+1)(2J'+1)]^{1/2} (W_{\Sigma} - W_{\Pi}) \begin{pmatrix} L & S & J \\ 0 & \Omega & -\Omega \end{pmatrix} \begin{pmatrix} L & S & J' \\ 0 & \Omega & -\Omega \end{pmatrix} \right]. \end{aligned} \quad (11)$$

TABLE I. Matrix elements of electronic plus spin-orbit Hamiltonian in body-frame basis.^a

	$ 00\rangle^a$	$ 20\rangle$	$ 10\rangle$
$ 00\rangle$	$\frac{1}{3}[2W_{\Pi}(R) + W_{\Sigma}(R)] - 2a(R)$	$\frac{\sqrt{2}}{3}[W_{\Pi}(R) - W_{\Sigma}(R)]$	0
$ 20\rangle$	$\frac{\sqrt{2}}{3}[W_{\Pi}(R) - W_{\Sigma}(R)]$	$\frac{1}{3}[W_{\Pi}(R) + 2W_{\Sigma}(R)] + a(R)$	0
$ 10\rangle$	0	0	$W_{\Pi}(R) - a(R)$
	$ 1\pm 1\rangle$	$ 2\pm 1\rangle$	
$ 1\pm 1\rangle$	$\frac{1}{2}[W_{\Pi}(R) + W_{\Sigma}(R)] - a(R)$	$\pm \frac{1}{2}[W_{\Pi}(R) - W_{\Sigma}(R)]$	
$ 2\pm 1\rangle$	$\pm \frac{1}{2}[W_{\Pi}(R) - W_{\Sigma}(R)]$	$\frac{1}{2}[W_{\Pi}(R) + W_{\Sigma}(R)] + a(R)$	
	$ 2\pm 2\rangle$		
$ 2\pm 2\rangle$	$W_{\Pi}(R) + a(R)$		

^aSee Eq. (11); the states are denoted $|J\Omega\rangle$ with $L=S=1$ understood.

$$\begin{aligned} \langle R, J'\Omega' | H_{MN}^0 | R, J\Omega\rangle &= \sum_{\substack{\Lambda\Lambda' \\ \Sigma\Sigma'}} (L \Lambda \Sigma | LSJ\Omega)(L \Lambda' \Sigma' | LSJ'\Omega') \\ &\times \langle R, \Lambda' \Sigma' | H_{MN}^0 | R, \Lambda \Sigma\rangle. \end{aligned} \quad (7)$$

Since

$$\langle R, \Lambda' \Sigma' | H_{MN}^0 | R, \Lambda \Sigma\rangle = \delta_{\Lambda\Lambda'} \delta_{\Sigma\Sigma'} W_{\Lambda\Sigma}(R), \quad (8)$$

it follows that the matrix elements vanish unless $\Omega = \Omega'$, so that Eq. (7) becomes

$$\begin{aligned} \langle J'\Omega' | H_{MN}^0 | J\Omega\rangle &= \delta_{\Omega\Omega'} [(2J+1)(2J'+1)]^{1/2} \\ &\times \sum_{\Lambda, \Sigma} \begin{pmatrix} L & S & J \\ \Lambda & \Sigma & -\Omega \end{pmatrix} \begin{pmatrix} L & S & J' \\ \Lambda & \Sigma & -\Omega \end{pmatrix} W_{\Lambda\Sigma}(R), \end{aligned} \quad (9)$$

where

$$\begin{pmatrix} L & S & J \\ \Lambda & \Sigma & -\Omega \end{pmatrix} \text{ and } \begin{pmatrix} L & S & J' \\ \Lambda & \Sigma & -\Omega \end{pmatrix}$$

are $3j$ symbols.

The spin-orbit interaction can be written as

$$W_{LS}(R) = a(R) \vec{L} \cdot \vec{S} = \frac{1}{2} a(R) [\vec{J}^2 - \vec{L}^2 - \vec{S}^2]. \quad (10)$$

Since the $|R, J\Omega\rangle$ functions are eigenfunctions of \vec{J}^2 , \vec{L}^2 , and \vec{S}^2 , it follows that the spin-orbit Hamiltonian is diagonal in the $|J\Omega\rangle$ basis. These diagonal terms can be added to Eq. (9) to give an expression for the matrix elements of the full electronic Hamiltonian [Eq. (1)]. Since the Born-Oppenheimer energies are independent of the signs of Λ and Σ , it is easy to show, using the orthogonality properties of the $3j$ symbols, that the summation over Λ and Σ in Eq. (9) can be evaluated analytically. This leads to the following expression:

Explicit expressions for these matrix elements are given in Table I.

We notice that in the $\Omega=0$ block the $J=1$ state is not coupled with either the $J=0$ or $J=2$ states. This is because the $3j$ symbols in Eq. (11) vanish when $L=S=J=1$ and $\Omega=0$. Since the $J=0$ state only appears in the $\Omega=0$ block, this implies that there is no coupling at all between the $J=0$ and $J=1$ levels (the $J=1$ and $J=2$ levels are coupled in the $\Omega=\pm 1$ blocks). The physical origin of this lack of coupling involves the symmetry of the wave functions with respect to reflection in a plane containing the M - N axis. The electrostatic potential H_{MN} is, of course, symmetric under this operation, and, for $\Omega=0$ the symmetry of the $|R, J\Omega\rangle$ functions is given by $(-1)^{J+1}$.²⁸ Thus within the $\Omega=0$ block, the even- J states will never be coupled with the odd- J states, regardless of the detailed nature of the electrostatic potential. Since the $J=0$ state only appears in the $\Omega=0$ block, it can thus never be coupled with any odd- J level. Alternatively, in line with the discussion given by Voronin and

Kvlividze¹⁴ or Cohen *et al.*,¹⁸ we can say that the $|J=2, \Omega=0\rangle$ and $|J=0, \Omega=0\rangle$ atomic states correlate with linear combinations of the ${}^3\Pi_{0-}$ and ${}^3\Sigma_{0-}$ molecular wave functions, while the $|J=1, \Omega=0\rangle$ atomic state correlates with the ${}^3\Pi_{0+}$ wave function.

Another formulation of the dynamics, which follows the initial approach of Reid and Dalgarno,^{3,4} is to expand the electrostatic Hamiltonian H_{MN}^0 [Eq. (2)] as an effective interaction involving only the lone p electron, namely,

$$H_{MN}^0(\vec{r}, \vec{R}) = \sum_{\lambda} V_{\lambda}(r, R) P_{\lambda}(\cos\theta), \quad (12)$$

where θ is the angle between \vec{r} , the vector describing the p electron, and \vec{R} . For the case of collisions involving an $nsn'p$ 3P atom, one can show, with a little angular momentum algebra, that only the $\lambda=0$ and $\lambda=2$ terms will contribute and that the body-frame matrix elements [Eq. (11)] are now given by

$$\begin{aligned} \langle J'\Omega' | H_{MN} | J\Omega \rangle = & \delta_{\Omega\Omega'} \left[\delta_{JJ'} \left[v_0(R) + \frac{a(R)}{2} [J(J+1) - L(L+1) - S(S+1)] \right] \right. \\ & \left. - (-1)^{J+J'-\Omega} [(6/5)(2J+1)(2J'+1)]^{1/2} \begin{Bmatrix} J & 2 & J' \\ -\Omega & 0 & \Omega \end{Bmatrix} \begin{Bmatrix} J & J' & 2 \\ 1 & 1 & 1 \end{Bmatrix} v_2(R) \right], \quad (13) \end{aligned}$$

where

$$\begin{Bmatrix} J & J' & 2 \\ 1 & 1 & 1 \end{Bmatrix}$$

is a $6j$ symbol and the $v_0(R)$ and $v_2(R)$ potentials are obtained by integrating the $V_0(r, R)$ and $V_2(r, R)$ terms over the coordinates of the p electron. The requirement of equivalency between Eqs. (11) and (13) implies, as previously derived by Aquilanti and Grossi,¹⁹

$$v_0(R) = [W_{\Sigma}(R) + 2W_{\Pi}(R)]/3 \quad (14)$$

and

$$v_2(R) = 5[W_{\Sigma}(R) - W_{\Pi}(R)]/3. \quad (15)$$

An expression for the body-frame potential matrix elements, analogous to Eq. (13), but for the case of collisions of 2P atoms, has been given by Fitz and Kouri.²⁵ As pointed out by Aquilanti and Grossi,¹⁹ Eq. (13) facilitates the connection between the present problem and the scattering of an atom by a rigid rotor, where $v_0(R)$ would be the spherically symmetric potential and $v_2(R)$, the anisotropy.

Up to this point we have expanded in body-frame states; the space-frame $|JM_J\rangle$ states are related to the $|J\Omega\rangle$ states by the transformation

$$|JM_J\rangle = \sum_{\Omega} D_{M_J, \Omega}^* (\theta, \phi, 0) |J\Omega\rangle, \quad (16)$$

where θ, ϕ describe the orientation of \vec{R} in the space

frame, and our definition of the Euler angles follows that of Brink and Satchler.²⁹ To describe the collision we expand the total wave function in eigenfunctions of the total angular momentum $\vec{J} = \vec{J} + \vec{I}$, where \vec{I} denotes the orbital angular momentum of the two-atom system. We have

$$|Jl\mathcal{J}M\rangle = \sum_{M_J, m_l} (JM_J m_l | Jl\mathcal{J}M) |JM_J\rangle |lm_l\rangle, \quad (17)$$

where the ket $|lm_l\rangle$ is a spherical harmonic. As discussed by Mies,⁵ the coupling scheme used corresponds to Hund's case (e).²⁷ The spherical harmonics in Eq. (17) can be expressed in terms of rotation matrix elements²⁹; the resulting product of two rotation matrix elements can be collapsed²⁹; and the sum over the M_J and m_l indices can be performed, using the orthogonality properties²⁹ of $3j$ symbols. We find

$$\begin{aligned} |Jl\mathcal{J}M\rangle = & [(2\mathcal{J}+1)(2l+1)/4\pi]^{1/2} (-1)^{\mathcal{J}} \\ & \times \sum_{\Omega} (-1)^{\Omega} \begin{Bmatrix} l & J & \mathcal{J} \\ 0 & \Omega & -\Omega \end{Bmatrix} D_{M, \Omega}^* |J\Omega\rangle. \quad (18) \end{aligned}$$

The matrix elements of the Hamiltonian $H_{MN} + V_{LS}$ can be evaluated from Eq. (18) by integration over all values of θ, ϕ and using Eq. (11). We find, after some straightforward angular momentum algebra,

$$\begin{aligned}
V_{J'l',Jl}(R) \equiv \langle J'l' \mathcal{J}M | H_{MN} | Jl \mathcal{J}M \rangle &= \delta_{JJ'} \delta_{ll'} \left[W_{\Pi} + \frac{a(R)}{2} [J(J+1) - L(9L+1) - S(S+1)] \right] \\
&+ [(2l+1)(2l'+1)(2J+1)(2J'+1)]^{1/2} (W_{\Sigma} - W_{\Pi}) \\
&\times \sum_{\Omega} \begin{bmatrix} l & J & \mathcal{J} \\ 0 & \Omega & -\Omega \end{bmatrix} \begin{bmatrix} l' & J' & \mathcal{J} \\ 0 & \Omega & -\Omega \end{bmatrix} \begin{bmatrix} L & S & J \\ 0 & \Omega & -\Omega \end{bmatrix} \begin{bmatrix} L & S & J' \\ 0 & \Omega & -\Omega \end{bmatrix}. \quad (19)
\end{aligned}$$

As in the case of the simpler body-frame potential [Eq. (11)], one can show from the restrictions on the $3j$ symbols in Eq. (19) that there is no coupling between the $J=0$ and $J=1$ states. Collision-induced transitions between these states will occur only through the second-order sequence $J=0, l=\mathcal{J} \rightarrow J=2, l=\mathcal{J}, \mathcal{J} \pm 2 \rightarrow J=1, l=\mathcal{J}$. As discussed by Aquilanti and Grossi,¹⁹ the space-frame potential matrix [Eq. (19)] for a given \mathcal{J} will separate because of parity into a 5×5 matrix involving states of parity $(-1)^{\mathcal{J}+1}$ and a 4×4 matrix involving states of parity $(-1)^{\mathcal{J}}$. An expression, equivalent to Eq. (19), for the space-frame potential in terms of the $v_0(R)$ and $v_2(R)$ terms [Eq. (13)] has been given by Aquilanti and Grossi.¹⁹

The total Hamiltonian for the collision can be written as

$$H = \frac{-\hbar^2}{2\mu} \nabla_R^2 + H_{MN}, \quad (20)$$

where H_{MN} is defined by Eq. (1). We will expand the total wave function in terms of the $|Jl \mathcal{J}M\rangle$ states as

$$U_{J'l',Jl}(R) = \frac{\hbar^2}{2\mu R^2} \langle J'l' \mathcal{J}M | \left[l_R^2 - l(l+1) - R^2 \frac{\partial^2}{\partial R^2} - 2R \frac{\partial}{\partial R} \right] | Jl \mathcal{J}M \rangle - \frac{\hbar^2}{2\mu} \langle J'l' \mathcal{J}M | \frac{\partial}{\partial R} | Jl \mathcal{J}M \rangle \frac{\partial}{\partial R}, \quad (24)$$

where $\vec{l}_R = \vec{\mathcal{J}} - \vec{J}$.

If these non-Born-Oppenheimer terms are neglected the coupled equations become entirely equivalent to those which appear in the treatment of atom-molecule rotationally inelastic scattering,³⁰ and which have been presented and solved by several authors^{3,4,6-13} in the case of collisions of atoms in 2P electronic states with noble-gas targets.

Furthermore, if the centrifugal term in Eq. (23) is replaced by a constant value $\bar{l}(l+1)/R^2$ for all channels, then, exactly as in the coupled-states (CS) approximation for rotationally inelastic collisions,^{31,32} a centrifugal decoupling of the CC equations can be achieved. This results in a block diagonalization in the index Ω with the potential matrix given by Eq. (11). Obviously, then, from the discussion following Eq. (11) we see that within this CS (j_z -conserving) approximation, there will be no coupling between the $J=0$ and $J=1$ states. The CC equations become reduced to three uncoupled equations ($J=2, \Omega=\pm 2$ and $J=1, \Omega=0$) and three sets of two coupled equations ($J=0, 2; \Omega=0$ and $J=1, 2; \Omega=\pm 1$). This quantum decoupling approximation has been applied to the study of fine-structure changing collisions by several different groups,^{10,18,20,21,25} apparently independently. Several semiclassical treatments containing a similar decoupling approximation have also appeared in the literature.^{1,26,33}

The CC equations (22) are solved subject to the bound-

$$\Psi(\vec{R}, \vec{r}) = \sum_{J,l,\mathcal{J},M} C_{Jl\mathcal{J}M}(R) | Jl \mathcal{J}M \rangle. \quad (21)$$

The $C_{Jl\mathcal{J}M}$ expansion coefficients satisfy the usual close-coupled (CC) equations

$$\begin{aligned}
\sum_{J',l'} [\delta_{ll'} \delta_{JJ'} D(R) + V_{J'l',Jl}(R)] C_{J'l'\mathcal{J}M}(R) \\
+ U_{J'l',Jl}(R) C_{J'l'\mathcal{J}M}(R) = 0, \quad (22)
\end{aligned}$$

where

$$D(R) = \frac{\hbar^2}{2\mu} \left[\frac{\partial^2}{\partial R^2} + \frac{2}{R} \frac{\partial}{\partial R} - \frac{l(l+1)}{R^2} \right] - E, \quad (23)$$

where E designates the total energy and $V_{J'l',Jl}(R)$ is defined by Eq. (19). The third term on the left-hand side (LHS) of Eq. (22) designates the so called non-Born-Oppenheimer terms and is written⁵

dary condition⁵

$$\begin{aligned}
\lim_{R \rightarrow \infty} C_{Jl\mathcal{J}M}(R) &= \delta_{JJ'} \delta_{ll'} \exp[-i(k_J R - \frac{1}{2} l' \pi)] \\
&- (k_{J'}/k_J)^{1/2} S_{J'l',Jl}^{\mathcal{J}} \\
&\times \exp[i(k_J R - \frac{1}{2} l \pi)], \quad (25)
\end{aligned}$$

where

$$k_J = [2\mu(E - E_{JnLS})/\hbar^2]^{1/2} \quad (26)$$

with the internal energy E_{JnLS} being defined by

$$\begin{aligned}
E_{JnLS} &= E_{nLS} + E_N + \frac{a(R=\infty)}{2} \\
&\times [J(J+1) - L(L+1) - S(S+1)]. \quad (27)
\end{aligned}$$

The inelastic cross section for the $J \rightarrow J'$ intramultiplet transition, averaged over projection quantum numbers, is given by the expression

$$\sigma_{J \rightarrow J'} = \frac{\pi}{k_J^2} \sum_{\mathcal{J}} P_{J \rightarrow J'}^{\mathcal{J}}, \quad (28)$$

where $P_{J \rightarrow J'}^{\mathcal{J}}$, the *weighted partial opacity*, is defined by

$$P_{J \rightarrow J'}^{\mathcal{J}} = \frac{(2\mathcal{J}+1)}{(2J+1)} \sum_{l,l'} |\delta_{JJ'} \delta_{ll'} - S_{J'l',Jl}^{\mathcal{J}}|^2. \quad (29)$$

In the CS approximation the scattering equations are

$$\sum_{J'} [\delta_{JJ'} \bar{D}(R) + V_{J'\Omega, J\Omega}(R)] C_{J'\Omega, \mathcal{F}M}(R) = 0, \quad (30)$$

where $\bar{D}(R)$ is defined by Eq. (23) with l replaced by \bar{l} . The potential matrix, which is independent of \bar{l} , is defined by Eq. (11) or, equivalently, by Eq. (13). These equations are solved subject to the boundary condition

$$\lim_{R \rightarrow \infty} C_{J'\Omega, \mathcal{F}M}(R) = \delta_{JJ'} \exp[-i(k_J R - \frac{1}{2} \bar{l} \pi)] - (k_{J'}/k_J)^{1/2} S_{J', J}^{\bar{l}\Omega} \times \exp[i(k_J R - \frac{1}{2} \bar{l} \pi)]. \quad (31)$$

The degeneracy-averaged integral cross sections are given in Eq. (28) with the weighted partial opacity defined either by the so-called $l = \mathcal{F}$ choice^{34,35}

$$P_{\mathcal{F} \rightarrow J'} = \frac{(2\mathcal{F}+1)}{(2J+1)} \sum_{\Omega} |\delta_{JJ'} - S_{J', \mathcal{F}}^{\bar{l}\Omega}|^2, \quad (32)$$

or by the $l = l_{\text{final}}$ choice^{34,35}

$$P_{\mathcal{F} \rightarrow J'} = \frac{1}{(2J+1)} \sum_{\Omega} \sum_l (2\bar{l}+1) (\bar{l}\Omega J' \Omega | \bar{l} J' \mathcal{F} \Omega)^2 \times |\delta_{JJ'} - S_{J', J}^{\bar{l}\Omega}|^2. \quad (33)$$

In the latter case, the range of \bar{l} values which contribute to the sum is restricted by the triangular relation contained in the Clebsch-Gordan coefficient. Equations (32) and (33) lead to identical expressions for the integral cross section.^{34,35}

III. POTENTIAL CURVES AND SCATTERING CALCULATIONS

Malvern²² has reported potential curves for a large number of electronic states of the Ca + He system, determined within an extension of the model potential method of Botcher.³⁶ Only the two outer electrons of the alkaline earth atom are considered explicitly; the remaining electrons and the two nuclei are treated as two polarizable cores. Explicit representations of the potential curves for

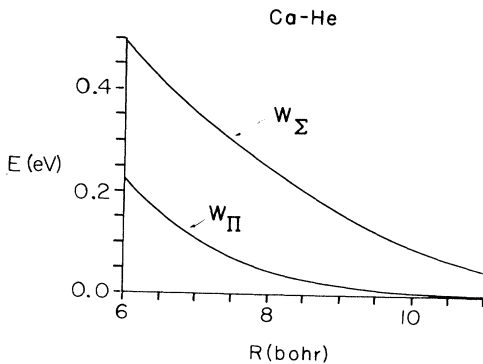


FIG. 1. Potential curves in eV for the $^3\Pi$ and $^3\Sigma^+$ electronic states arising from the interaction of a Ca atom in the $4s4p\ ^3P$ electronic state with a He atom, as determined by Malvern (Refs. 22 and 37). The curves correspond to the quantities $W_{\Lambda\Sigma nLS}(R)$ defined by Eq. (3).

the $^3\Pi$ and $^3\Sigma$ states which correlate asymptotically with $\text{Ca}(^3P) + \text{He}$ were obtained by a spline fit of Malvern's tabulated values.^{22,37} Figure 1 displays the dependence on R of W_{Σ} and W_{Π} for the Ca-He system. At values of R less than 5 bohr, Malvern's curves were continued using exponential extrapolations. We observe that the Σ curve is considerably more repulsive. This is because the Ca $4p$ orbital lies along the internuclear axis in the Σ state, and thus experiences a more repulsive interaction with the filled helium $1s$ shell.

If we refer to the formulation of the collision in terms of a spherically symmetric potential and a $P_2(\cos\theta)$ anisotropy [Eq. (13)], we see from Eqs. (14) and (15) that at moderate to large values of R the effective anisotropy will be much larger than the spherically symmetric term. This should be contrasted, obviously, with the case of atom-rotor collisions, where the anisotropies are in general significantly smaller than the spherical component of the potential.

The CC and CS equations were solved using, respectively, the logarithmic derivative^{38,39} and renormalized Numerov^{40,41} algorithms developed by Johnson. The spin-orbit constant $a(R)$ in Eq. (19) was assumed to be independent of R and was taken equal to the value appropriate to the $\text{Ca}(^3P)$ atom, 52.5 cm^{-1} .⁴²

IV. RESULTS

Before presenting the results of our calculations, it will be worthwhile to discuss first the expected magnitude and behavior of the cross sections, based on conclusions derived from earlier studies of intramultiplet transitions. As indicated in Table I, the coupling between the various spin-orbit states is proportional to the splitting between the $^3\Pi$ and $^3\Sigma$ potential curves, which, as we see in Fig. 1, is large. A rough fit of $W_{\Sigma} - W_{\Pi}$ to an exponential indicates that the range of the coupling potential, ρ , is on the order of 1–1.5 Å. The Massey parameter, defined as^{1,14,43}

$$\xi = (\Delta E / \hbar) / (v / \rho), \quad (34)$$

where ΔE is the fine-structure splitting, and v is the velocity of the Ca atom relative to the noble gas, will be on the order of unity for Ca-He collisions at the relative velocities which characterize the experiments of Yuh and Dagdigan.²⁴ Thus the collisions are neither adiabatic ($\xi \gg 1$), nor sudden ($\xi \ll 1$). Since we are not in the adiabatic limit we expect fairly large cross sections.

Of particular interest will be the accuracy of the CS (j_z -conserving) approximation. If the scattering is dominated purely by first-order electrostatic coupling, then, as discussed in Sec. II, we would expect the $J=0 \rightarrow 1$ cross section to be considerably smaller than the $J=0 \rightarrow 2$, $1 \rightarrow 2$ values, since the $J=0$ and $J=1$ levels are not directly coupled by the electrostatic potential. This prediction would be consistent with the experimental intramultiplet rates for collisions of CH_4 with $\text{Cd}(^3P)$ and $\text{Sn}(^3P)$ reported by, respectively, Breckenridge and Malmin⁴⁴ and by Husain, Wiesenfeld, and co-workers.⁴⁵ As we have seen in Sec. II, the coupling with the rotational motion of the nuclei does allow the $J=0$ and $J=1$ levels to mix by means of the $J=2$ level. Thus, if the $J=0 \rightarrow 2$ and $1 \rightarrow 2$ coupling is strong, we would expect significant $J=0 \rightarrow 1$ cross sections, arising from second- and higher-

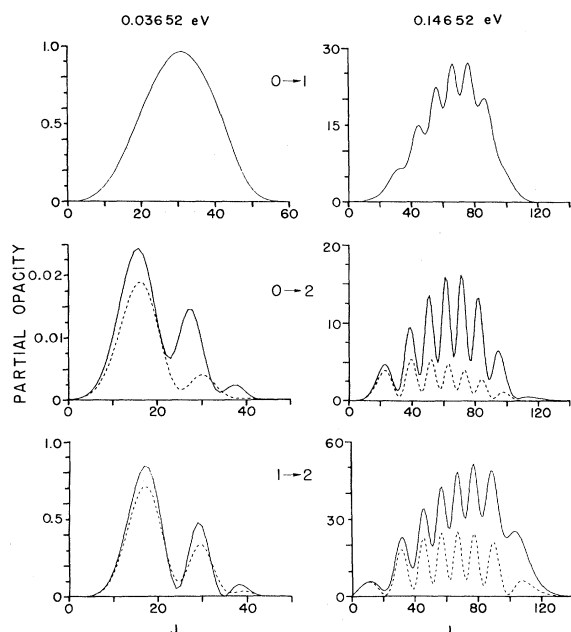


FIG. 2. Weighted partial opacity curves [Eq. (29)] as a function of the total angular momentum for collisions of $\text{Ca}(^3P)$ with He at total energies of 0.146515 eV and 0.036515 eV. The CS (j_z -conserving) curves (dashed lines) were calculated with the l -final definition of the partial opacity [Eq. (33)]. Within the CS approximation the $0 \rightarrow 1$ transition is forbidden.

order processes. Physically this would imply a strong degree of coupling between the rotational motion of the nuclei and of the p electron on the alkaline-earth atom.

The model studies of Aquilanti and co-workers²⁰ suggest that the CS approximation will not be accurate whenever the fine-structure splitting is small, but not negligible. Also, the study by Fitz and Kouri²⁵ of Na-He collisions at 0.04 eV indicates that the accuracy of the CS approximation may be dependent on the particular choice of interaction potential.

Figure 2 displays the weighted partial opacity curves for

Ca-He collisions at total energies of 0.146515 eV and 0.036515 eV which are equivalent, respectively, to translational energies of 0.14 eV and 0.03 eV in the $J=1$ channel. These values straddle the range of translational energies sampled in the beam-gas experiments of Yuh and Dagdigan.²⁴ We recall that the $(J=0)-(J'=1)$ splitting is 0.0064 eV and the 1-2 splitting, 0.0130 eV.⁴² For both energies, the values of J beyond which the opacity curves fall to zero correspond roughly to the semiclassical value of the impact parameter for which the electrostatic coupling, $W_{\Sigma} - W_{\Pi}$ (Table I), becomes equal in magnitude to the average splitting between the three fine-structure levels.

The pronounced oscillatory structure in the partial opacity curves, similar to that seen for collisions of various alkali-metal-noble-gas pairs,^{4,8,25} especially in the case of strong-coupling potentials, reflects the strength of the electrostatic coupling. As we have discussed in the preceding section, the anisotropy in the effective-coupling potential [Eq. (15)] is much larger than the spherically symmetric term. We note that the amplitude of the oscillations is less pronounced for the $0 \rightarrow 1$ transition. Since these two states are not directly coupled, the transition must proceed through various intermediate states, which will tend to damp out the oscillatory structure. At the lower energy the de Broglie wavelength of the system is now considerably larger, so, as we might expect, there are now only a few oscillations in the $0 \rightarrow 2$ and $1 \rightarrow 2$ partial opacity curves, and none in the $0 \rightarrow 1$ curve.

The structure in the CS and CC partial opacity curves agrees reasonably well for both the $0 \rightarrow 2$ and $1 \rightarrow 2$ transitions, although, as observed by Fitz and Kouri²⁵ in the case of Na-He collisions, the minima in the CS partial opacities are deeper.

Table II lists both CC and CS integral cross sections at a variety of energies. As expected, the cross sections rise rapidly as the energy increases. To investigate more clearly this energy dependence we plot in Fig. 3 the CC *deexcitation* cross sections $2 \rightarrow 1$, 0 , and $1 \rightarrow 0$ as a function of initial translational energy. The $2 \rightarrow 1$ transition is clearly the strongest, at all energies. We see that despite the absence of direct coupling the calculated cross sections for the $1 \rightarrow 0$ transition are much larger than those for the $2 \rightarrow 0$ transition. The dominance of $1 \rightarrow 0$ process may reflect an energy gap which is a factor of 3 smaller than the

TABLE II. Intramultiplet integral cross sections (in \AA^2) for collisions of $\text{Ca}(^3P)$ with He. Exponents for multiplicative factors of 10 are enclosed within parentheses.

E (eV) ^a	Transition					
	$0 \rightarrow 1^b$		$0 \rightarrow 2$		$1 \rightarrow 2$	
	CC	CS	CC	CS	CC	CS
0.01401528	1.17(-2)	c	c	c	c	c
0.02151528	1.14(-1)	3.45(-6)	1.43(-6)	2.31(-3)	2.35(-3)	
0.02651528	3.38(-1)	5.49(-4)	4.29(-4)	9.40(-2)	4.25(-2)	
0.03651528	1.18	1.75(-2)	1.14(-2)	6.29(-1)	5.51(-1)	
0.05651528	3.79	3.15(-1)	1.56(-1)	4.61	2.82	
0.08151528	7.45	1.48	5.94(-1)	13.76	6.61	
0.14651528	15.27	7.67	2.76	35.67	15.15	
0.30651528	24.22	25.43	9.69	58.82	28.95	

^aTotal energy in eV.

^bCS cross sections are identically zero for this transition.

^cThe $J=2$ channel is closed at this energy.

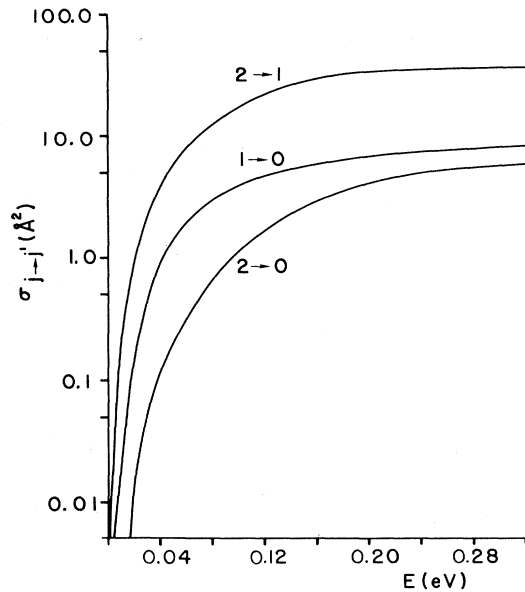


FIG. 3. CC deexcitation cross sections for $\text{Ca}(^3P_J)+\text{He}$ collisions as a function of the translational energy in the initial (higher-energy) channel.

$2 \rightarrow 0$ gap. At high energy this consideration will become irrelevant, so that the difference between the $1 \rightarrow 0$ and $2 \rightarrow 0$ cross sections should become less pronounced, which is what we see in Fig. 3. Also, another explanation of the larger size of the $1 \rightarrow 0$ cross section, relative to the $2 \rightarrow 0$ value, is that the $1 \rightarrow 0$ transition represents the only exoergic relaxation pathway for the $J=1$ level, while two such transitions ($2 \rightarrow 1$ and $2 \rightarrow 0$) exist for the $J=2$ level. Eventually, at very low translational energies, we might expect to enter a regime in which the collision could be adequately described by the first-order Born approximation, in which case the $1 \rightarrow 0$ transition would become forbidden. However, we see no indication in Fig. 3 of where this regime might begin.

The agreement between the CC and CS cross sections is reasonable, although the CS values are consistently too small, often by a factor of 2 or greater. Since the CC $0 \rightarrow 1$ cross sections are so large (relative to the $0 \rightarrow 2$ and $1 \rightarrow 2$ values), it is clear that the rotational (Coriolis) coupling between the nuclear and the electronic rotation must be an important effect. To neglect this, as is done in the CS approximation, results here in the introduction of considerable error, even for the transitions ($0 \rightarrow 2, 1 \rightarrow 2$), which are coupled by the electrostatic potential. The comparison, done by Fitz and Kouri,²⁵ of CC and CS cross sections for intramultiplet transitions in $\text{Na}(^2P)+\text{He}$ collisions was considerably more favorable than the present one. As discussed in the Introduction, Cohen, Collins, and Lane¹⁸ have published CS cross sections for $\text{Ne}(^3P)+\text{Ne}(^1S)$ collisions. In light of the present article, it would be interesting to compare their cross sections with the results of a full CC treatment on the same system.

It is interesting to compare our calculated cross sections with the predictions of simple statistical or scaling theories. The simplest statistical model would predict at

high energy⁴⁶

$$\sigma_{J \rightarrow J'} \sim (2J' + 1). \quad (35)$$

This prediction clearly does not apply well to the present system. As an example, the $0 \rightarrow 2$ cross sections are predicted to be $\frac{5}{3}$ as large as the $0 \rightarrow 1$ values, which is not substantiated by the CC values listed in Table II. Recently, Kouri and co-workers⁴⁷ have demonstrated the utility, in the study of rotationally inelastic collisions, of the scaling relations which can be derived within an energy sudden limit.⁴⁸ The cross sections for transitions between any two rotational levels can be expressed in terms of the cross sections out of the $J=0$ level, as given by the following expression⁴⁷:

$$\sigma_{J \rightarrow J'} = \frac{k_0^2}{k_J^2} (2J' + 1) \sum_{\bar{J}} \begin{bmatrix} J & \bar{J} & J' \\ 0 & 0 & 0 \end{bmatrix}^2 \sigma_{0 \rightarrow \bar{J}}. \quad (36)$$

If we apply this relation to the present problem we predict the following relation between the $2 \rightarrow 1$ and $1 \rightarrow 0$ cross sections at high energy, where the sudden limit might be expected to be valid:

$$\sigma_{2 \rightarrow 1} = 1.2 \sigma_{1 \rightarrow 0}. \quad (37)$$

We see from Fig. 3 that the actual ratio is considerably greater.

V. ADIABATIC INTERPRETATION

An interesting interpretation of the inelastic coupling is possible within a model which treats the nuclear motion adiabatically, which has been used^{1,14,26} in semiclassical treatments of intramultiplet transitions, principally in collisions of 2P atoms.⁴⁹ In this approach, we first define a new potential matrix which combines the electrostatic and spin-orbit potential matrix [$V_{J'l, J'l}(R)$ in Eq. (22)] with the nuclear orbital angular momentum, namely,

$$W_{J'l, J'l}^f(R) = \delta_{J'l, J'l} \frac{\hbar^2 l(l+1)}{2\mu R^2} + V_{J'l, J'l}^f(R). \quad (38)$$

Then, linear combinations of the $|Jl \mathcal{M}\rangle$ states [Eqs. (17) and (18)] are taken to diagonalize the W^f matrix. These new eigenvectors are designated $|n \mathcal{M}\rangle$, where

$$|n \mathcal{M}\rangle = \sum_{J,l} A_{n, Jl}(R) |Jl \mathcal{M}\rangle, \quad (39)$$

and the coefficients $A_{n, Jl}(R)$ are chosen so that

$$\begin{aligned} W_{n', n}^f(R) &= \sum_{J, l, J', l'} A_{n', J'l'}^*(R) A_{n, Jl}(R) W_{J'l, J'l}^f(R) \\ &= \delta_{n'n} \Lambda_n^f(R). \end{aligned} \quad (40)$$

The $|n \mathcal{M}\rangle$ are called adiabatic states.

The scattering wave function can be expanded in terms of these states, in a manner similar to Eq. (21). We write

$$\Psi(\vec{R}, \vec{r}) = \sum_{n, \mathcal{M}} \frac{1}{R} U_n^{\mathcal{M}}(R) |n \mathcal{M}\rangle. \quad (41)$$

If one neglects all the non-Born-Oppenheimer terms [Eq. (24)], which couple the nuclear with the electronic motion, then the CC equations (22) become

$$\sum_n \left[\delta_{nn'} \left[-\frac{\hbar^2}{2\mu} \frac{d^2}{dR^2} + \Lambda_{n'}^{\mathcal{J}} - E \right] U_{n'}^{\mathcal{J}M}(R) - \frac{\hbar^2}{\mu} G_{n'n}^{\mathcal{J}}(R) \frac{d}{dR} U_n^{\mathcal{J}M}(R) - \frac{\hbar^2}{2\mu} F_{n'n}^{\mathcal{J}}(R) U_n^{\mathcal{J}M}(R) \right] = 0, \quad (42)$$

where

$$G_{n'n}^{\mathcal{J}}(R) = \sum_{J,l} A_{n',Jl}^*(R) \frac{d}{dR} A_{n,Jl}(R), \quad (43)$$

and

$$F_{n'n}^{\mathcal{J}}(R) = \sum_{J,l} A_{n',Jl}^*(R) \frac{d^2}{dR^2} A_{n,Jl}(R). \quad (44)$$

These two matrices can be determined by numerical differentiation of the matrix of eigenvectors.

In this adiabatic formulation each $|n\mathcal{J}M\rangle$ state correlates asymptotically with a particular $|Jl\mathcal{J}M\rangle$ state, so that inelastic intramultiplet transitions arise solely from the off-diagonal terms in the $F^{\mathcal{J}}$ and $G^{\mathcal{J}}$ matrices. In Fig. 4, we illustrate the R dependence of the off-diagonal $G^{\mathcal{J}}$ matrix elements which correspond to the coupling between different spin-orbit states. The $F^{\mathcal{J}}$ matrix elements were found to be considerably smaller in magnitude, as is often assumed in the theory of nonadiabatic processes.⁵⁰ The variation with \mathcal{J} was found to be small in the case of the $G^{\mathcal{J}}$ matrix elements corresponding to $(J=0)-(J'=2)$ and $(J=1)-(J'=2)$ coupling, but much larger in the case of the matrix element corresponding to $(J=0)-(J'=1)$ coupling. This is because, as discussed above, the $(J=0)-(J'=1)$ mixing arises only through coupling of the electronic and nuclear angular momenta, and so will become

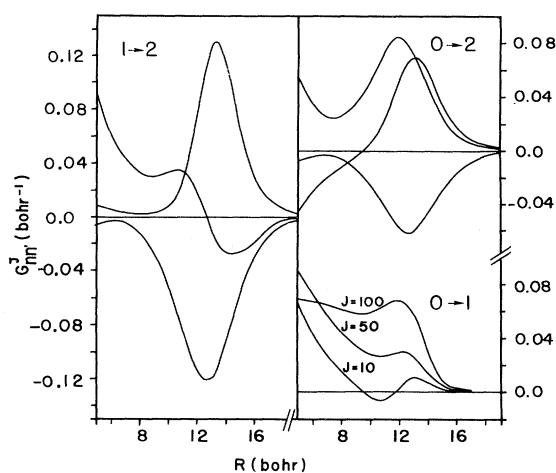


FIG. 4. Dependence on internuclear separation of the nonadiabatic coupling matrix elements [Eq. (43)] for those transitions which correspond asymptotically to transitions between the indicated fine-structure levels. In all cases the initial and final $|n\mathcal{J}M\rangle$ states [Eq. (39)] have odd parity. For the 0-1 and 1-2 matrix elements the value of \mathcal{J} is 20; for the 0-1 matrix elements the three values of \mathcal{J} used are listed. The ordinate on the left refers to the 1-2 matrix elements; the ordinate on the right, to the 0-1 and 0-2 matrix elements.

more important as \mathcal{J} and, consequently, l increase.

We see that there are two fairly distinct regions of large nonadiabaticity. Following the spirit of the discussion by Aquilanti and Grossi,¹⁹ we can interpret these two regions by means of an analysis based on various Hund's case coupling limits. The first region of large nonadiabatic coupling, at large R , occurs at the transition between the asymptotic region, where the spin-orbit splitting dominates the electrostatic interaction and a Hund's case (e) limit is appropriate, and a region where the electrostatic interaction is dominant and a case (a) limit is appropriate. Indeed, the first maxima in the nonadiabatic coupling in Fig. 4 occurs at $R \approx 13$ bohr, which corresponds fairly closely to the point at which the electrostatic coupling, $W_{\Sigma} - W_{\Pi}$ (Table I), becomes equal in magnitude to the average splitting between the three $\text{Ca}(^3P)$ fine-structure levels. At smaller R the nonadiabatic coupling again increases, marking the transition between the case (a) region, where the centrifugal potential is nondiagonal, to a region at very small R , where the centrifugal potential dominates the electrostatic interaction. Unfortunately, since Malvern's calculations do not extend beyond $R = 5$ bohr, it was not possible to look quantitatively at the nonadiabatic coupling in this small- R region.

We also observe from Fig. 4 that the region of nonadiabatic coupling extends over a considerably larger range of R values than in the case of $\text{F}(^2P) + \text{Xe}$ collisions, treated by Miller *et al.*²⁶ Furthermore, since there is substantial overlap between the regions of strong nonadiabatic coupling between the individual spin-orbit states, it would probably not be accurate, at least for $\text{Ca}(^3P) + \text{He}$ collisions, to use a simplified two-state model to determine cross sections for the three independent $J \rightarrow J'$ transitions.

VI. COMPARISON WITH EXPERIMENT

In the preceding article, Yuh and Dagdigan²⁴ have described a two-laser experiment to measure intramultiplet rate constants for intramultiplet transfer in $\text{Ca}(^3P) + \text{He}$ collisions. The velocity-averaged cross sections obtained from the experiment can be related to the theoretically determined quantities by integration over the appropriate flux distribution. We have⁵¹

$$\bar{\sigma}_{J \rightarrow J'} = \int \sigma_{J \rightarrow J'}(v) v f(v) dv / \int v f(v) dv, \quad (45)$$

where $f(v)$ is the experimental velocity distribution. Equivalently, this may be written as an integral over the relative translational energy, namely,

$$\bar{\sigma}_{J \rightarrow J'} = \int \sigma_{J \rightarrow J'}(E) E^{1/2} f(E) dE / \int E^{1/2} f(E) dE. \quad (46)$$

For the particular experimental conditions of Yuh and Dagdigan, the distribution of relative translational energies is plotted in Fig. 7 of Ref. 24. As can be seen, from comparison with Fig. 3 and Table II, this type of beam-gas experiment samples a broad range of translational energies over which the actual Ca-He cross sections are changing by many orders of magnitude.

By using a power law to interpolate between the computed CC cross sections, we were able to carry out the integration of Eq. (46) numerically to obtain the values shown in Table III. The overall agreement is poor, consid-

TABLE III. Velocity-averaged intramultiplet integral cross sections (in \AA^2) for collisions of $\text{Ca}(^3P)$ with He.

J	J'	Theory ^b	$\bar{\sigma}_{J \rightarrow J'}$ ^a	Experiment ^c
2	1	11.2		31.9 ± 4.2
2	0	0.78		5.5 ± 1.6
1	0	2.5		2.0 ± 5.0

^aEquations (45) and (46) of text.

^bObtained from numerical integration of Eq. (46) with experimentally determined $f(E)$ (Fig. 7 of Ref. 24) and power-law interpolation of the CC cross sections (see Table II).

^cReference 24; the indicated errors correspond to one standard deviation.

erably worse than the degree of agreement between the experimental intramultiplet rate constants reported for the $\text{Na}(^2P) + \text{He}$ system⁵² and the CC cross sections calculated by Reid,⁴ using the potential curves of Baylis.⁵³ We note that these curves were determined with a pseudopotential method analogous to that used by Malvern²² to determine the Ca-He potential curves. We observe that the experiments confirm the prediction of a sizable value for the $1 \rightarrow 0$ cross section, despite the absence of electrostatic coupling between these two levels. However, the experimental values for the $2 \rightarrow 1$ and $2 \rightarrow 0$ cross sections are three-to-four times larger than the calculated theoretical values. Also there is a significant discrepancy between the theoretical and experimental values for the ratio of the $1 \rightarrow 0$ and $2 \rightarrow 0$ cross sections.

Hopefully this disagreement would be resolved if the Ca-He interaction were treated at a more exact *ab initio* level, rather than with the two-electron pseudopotential method used by Malvern.²² Extensive studies^{4,8} of the $\text{Na}(^2P) + \text{He}$ system have shown how intramultiplet cross sections can be very sensitive to the assumed potential curves. It is intriguing to speculate that the magnitude of the cross sections and the ratio of the $1 \rightarrow 0$ and $2 \rightarrow 0$ values will be a sensitive function of the chosen potential curves. Since the theoretical cross sections rise rapidly over the range of translational energies sampled in the experiment of Yuh and Dagdigian (see Fig. 3 of the present paper and Fig. 7 of Ref. 24), additional information on the dynamics could be furnished by further experiments which would probe the energy dependence⁵⁴ of all three intramultiplet cross sections.

VII. CONCLUSION

We have described the quantum formulation of the dynamics of collisions between atoms in 3P electronic states and structureless partners and have reported calculations of intramultiplet cross sections for collisions of $\text{Ca}(^3P)$ with He, carried out using the potential curves determined by Malvern.²² Both full close-coupling (CC) and coupled-states (j_z -conserving) calculations were carried out. Our major conclusions are as follows.

(1) The inelastic cross sections rise rapidly with increasing energy.

(2) Despite the absence of direct electrostatic coupling between the $J=0$ and $J=1$ levels, the strength of the

$J=0 \rightarrow 2$ and $J=2 \rightarrow 1$ coupling is such that the $J=0 \rightarrow 1$ cross sections are comparable in magnitude to those for the directly coupled $1 \rightarrow 2$ transition and significantly larger than those for the $0 \rightarrow 2$ transition. This higher-order $J=0 \rightarrow J'=1$ coupling occurs because of the coriolis coupling between the orbital and electronic angular momenta.

(3) Because this coriolis coupling is specifically neglected within the CS approximation, the CS cross sections differ considerably from the exact CC values. For the $0 \rightarrow 2$ and $1 \rightarrow 2$ transitions, which are allowed within the CS approximation, the cross sections appear to be accurate within roughly a factor of 2.

(4) The agreement is not good between our calculated Ca-He cross sections and the experimental rate constants reported by Yuh and Dagdigian.²⁴ The major disagreement is the magnitude of the $2 \rightarrow 1$ and $2 \rightarrow 0$ cross sections and the ratio of the smaller $1 \rightarrow 0$ and $2 \rightarrow 0$ cross sections.

It would be particularly interesting to extend the present study to collisions of $\text{Ca}(^3P)$ with other noble gas partners. In the case of Ar, we would expect a deep well in the $^3\Pi$ potential curve, at least judging from experimentally determined $\text{Na}(^2P) + \text{Ar}$ and $\text{K}(^2P) + \text{Ar}$ potential curves.⁵⁵ Consequently, $W_\Sigma - W_\Pi$ (Table I) would be large, which might imply a large degree of intramultiplet mixing. Also, one could investigate collisions of other 3P atoms, which would allow some exploration of the sensitivity of the intramultiplet cross sections to the size of the spin-orbit splitting. An obvious candidate is $\text{Mg}(^3P) + \text{He}$, Ne for which potential curves already exist.^{22,23}

It is clear that the study of intramultiplet transitions in collisions of 3P atoms provides an additional richness not found in the alkali-metal series, due to the triplet multiplicity. The present investigation, and the comparison with the experimental results reported in the preceding article,²⁴ indicate that both the absolute and relative magnitudes of the intramultiplet rates will provide a sensitive probe of the interatomic potentials and the details of the collision dynamics. Further, *ab initio* work is clearly needed, to provide a more accurate description of the $\text{Ca}(^3P) + \text{He}$ interaction potentials. Accurate quantum calculations, such as the ones presented here, can provide not only valuable comparisons with future experiments, but also standards for calibration as well as incentives for development of appropriate semiclassical^{14-16,26,33} and quantum^{17,18,20,25} approximation techniques.

ACKNOWLEDGMENTS

Support for this work was provided by the U.S. Army Research Office, Grant No. DAAG29-81-K-0102, by the Computer Science Center of the University of Maryland, by North Atlantic Treaty Organization under research Grant No. 232.81, and by the French Centre National de la Recherche Scientifique under ATP No. 1137. We are indebted to our experimentalist colleagues, Huoy-Jen Yuh and Paul Dagdigian, who provided the inspiration for the present study. One of us (M.H.A.) would like to thank Alexander Reznikov, Stanislav Umanskii, and Evgeny Nikitin for a very instructive tutorial on the theory of fine-structure-changing collisions.

- *Permanent address: Institute of Physics, Nicholas Copernicus University, PL-87-100 Toruń, Poland
- †Present address: Department of Chemistry, Columbia University, New York, NY 10027
- ¹E. E. Nikitin, *J. Chem. Phys.* **43**, 744 (1965); *Adv. Chem. Phys.* **28**, 317 (1975).
 - ²E. E. Nikitin and A. I. Reznikov, *J. Phys. B* **13**, L57 (1980); A. I. Reznikov, *ibid.* **15**, L157 (1982), and references contained therein.
 - ³R. H. G. Reid and A. Dalgarno, *Phys. Rev. Lett.* **22**, 1029 (1969); *Chem. Phys. Rev. Lett.* **6**, 85 (1970).
 - ⁴R. H. G. Reid, *J. Phys. B* **6**, 2018 (1973).
 - ⁵F. H. Mies, *Phys. Rev. A* **7**, 942 (1973).
 - ⁶F. H. Mies, *Phys. Rev. A* **7**, 957 (1973).
 - ⁷J. C. Weisheit and N. F. Lane, *Phys. Rev. A* **4**, 171 (1971).
 - ⁸A. D. Wilson and Y. Shimoni, *J. Phys. B* **7**, 1543 (1974); **8**, 1392 (1975); **8**, 2393 (1975).
 - ⁹R. E. Olson, *Chem. Phys. Lett.* **33**, 250 (1975); R. P. Saxon, R. E. Olson, and B. Liu, *J. Chem. Phys.* **67**, 2692 (1977).
 - ¹⁰J. M. Launay and E. Roueff, *J. Phys. B* **10**, 879 (1977).
 - ¹¹C. H. Becker, P. Casavecchia, Y. T. Lee, R. E. Olson, and W. A. Lester, Jr., *J. Chem. Phys.* **70**, 5477 (1979).
 - ¹²J. Pascale and M. Y. Perrin, *J. Phys. B* **13**, 1839 (1980).
 - ¹³R. W. Anderson, *J. Chem. Phys.* **77**, 5426 (1982).
 - ¹⁴A. I. Voronin and V. A. Kvlivdize, *Theor. Chim. Acta* **8**, 334 (1967).
 - ¹⁵M. A. D. Fluendy, I. H. Kerr, and K. P. Lawley, *Mol. Phys.* **28**, 69 (1974).
 - ¹⁶A. Z. Devdariani and I. I. Zagrebin, *Zh. Fiz. Khim.* (in press).
 - ¹⁷S. Wofsy, R. H. G. Reid, and A. Dalgarno, *Astrophys. J.* **168**, 161 (1971); A. W. Yau and A. Dalgarno, *ibid.* **206**, 652 (1976).
 - ¹⁸J. S. Cohen, L. A. Collins, and N. F. Lane, *Phys. Rev. A* **17**, 1343 (1978).
 - ¹⁹V. Aquilanti and G. Grossi, *J. Chem. Phys.* **73**, 1165 (1980).
 - ²⁰V. Aquilanti, P. Casavecchia, G. Grossi, and A. Laganà, *J. Chem. Phys.* **73**, 1173 (1980).
 - ²¹V. Aquilanti, G. Grossi, and A. Laganà, *Nuovo Cimento* **63B**, 7 (1981).
 - ²²A. R. Malvern, *J. Phys. B* **11**, 831 (1978).
 - ²³I. N. Demetropoulos and K. P. Lawley, *J. Phys. B* **15**, 1855 (1982).
 - ²⁴H.-J. Yuh and P. J. Dagdigian, *Phys. Rev. A* **28**, 63 (1983), preceding paper.
 - ²⁵D. E. Fitz and D. J. Kouri, *J. Chem. Phys.* **73**, 5115 (1980).
 - ²⁶R. K. Preston, C. Sloane, and W. H. Miller, *J. Chem. Phys.* **60**, 4961 (1974).
 - ²⁷G. Herzberg, *Spectra of Diatomic Molecules*, 2nd ed. (Van Nostrand, Princeton, 1950).
 - ²⁸The symmetry follows directly from the discussion given by J. T. Hougen [Natl. Bur. Stand. (U.S.) Monogr. **115** (1970)].
 - ²⁹D. M. Brink and G. R. Satchler, *Angular Momentum*, 2nd ed. (Oxford University, Oxford, England, 1975).
 - ³⁰A. M. Arthurs and A. Dalgarno, *Proc. R. Soc. London* **A256**, 540 (1960).
 - ³¹P. McGuire and D. J. Kouri, *J. Chem. Phys.* **60**, 2488 (1974); R. T. Pack, *ibid.* **60**, 633 (1974).
 - ³²D. J. Kouri, in *Atom-Molecule Collision Theory: A Guide for the Experimentalist*, edited by R. B. Bernstein (Plenum, New York, 1979), p. 301.
 - ³³C. Bottcher, *J. Phys. B* **9**, 3099 (1976).
 - ³⁴R. T. Pack, *J. Chem. Phys.* **66**, 1557 (1977).
 - ³⁵Y. Shimoni and D. J. Kouri, *J. Chem. Phys.* **66**, 2841 (1977).
 - ³⁶C. Bottcher *J. Phys. B* **4**, 1140 (1971); C. Bottcher and A. Dalgarno, *Proc. R. Soc. London* **A340**, 187 (1974).
 - ³⁷See footnote on p. 840 of Ref. 22.
 - ³⁸B. R. Johnson, *J. Comput. Phys.* **13**, 445 (1973).
 - ³⁹B. R. Johnson, *National Resource for Computation in Chemistry Software Catalog*, Prog. No. KQ06 (LOGD), 1980, obtainable from the Quantum Chemistry Program Exchange, Department of Chemistry, Indiana Univ., Bloomington, IN 47405.
 - ⁴⁰B. R. Johnson, *J. Chem. Phys.* **67**, 4086 (1977).
 - ⁴¹B. R. Johnson, in *Proceedings of the NRCC Workshop on Algorithms and Computer Codes for Atomic and Molecular Scattering Theory*, edited by L. D. Thomas, 1979, Vol. 1, pp. 86–104. Available as document LBL-9501, UC-4, CONF-790696 (unpublished) from National Technical Information Service, U.S. Department of Commerce, 5285 Port Royal Rd., Springfield, VA 22161.
 - ⁴²C. E. Moore, *Atomic Energy Levels*, National Stand. Ref. Data Ser. **35**, 1971, Vol. I, p. 243 (National Bureau of Standards, Washington, D.C., 1971).
 - ⁴³M. S. Child, *Molecular Collision Theory (Academic, New York, 1974)*, p. 88.
 - ⁴⁴W. H. Breckenridge and O. K. Malmin, *J. Chem. Phys.* **76**, 1812 (1982).
 - ⁴⁵P. D. Foo, J. R. Wiesenfeld, M. J. Yuen, and D. Husain, *J. Phys. Chem.* **80**, 95 (1976).
 - ⁴⁶See, for example, R. D. Levine, R. B. Bernstein, P. Kahana, I. Procaccia, and E. T. Upchurch, *J. Chem. Phys.* **64**, 796 (1976).
 - ⁴⁷R. Goldflam, D. J. Kouri, and S. Green, *J. Chem. Phys.* **67**, 5661 (1977); R. Goldflam and D. J. Kouri, *ibid.* **70**, 5076 (1979); Z. H. Top and D. J. Kouri, *Chem. Phys.* **37**, 2651 (1979).
 - ⁴⁸M. H. Alexander, *J. Chem. Phys.* **71**, 5212 (1979).
 - ⁴⁹A similar approach has been used by Takayanagi and co-workers to treat rotationally inelastic molecular collisions. For the quantum formulation, see K. Takayanagi, Institute for Space and Aeronautical Sciences (University of Tokyo), Research Note No. 51 (unpublished); K. Sakimoto, Research Note No. 125 (unpublished).
 - ⁵⁰J. C. Tully, in *Modern Theoretical Chemistry*, edited by W. H. Miller (Plenum, New York, 1976), Vol. 2, p. 217.
 - ⁵¹See, for example, L. Pasternack and P. J. Dagdigian, *J. Chem. Phys.* **67**, 3854 (1977).
 - ⁵²J. A. Jordan and P. A. Franken, *Phys. Rev.* **142**, 20 (1966); J. Pitre and L. Krause, *Can. J. Phys.* **45**, 2671 (1967).
 - ⁵³W. E. Baylis, *J. Chem. Phys.* **51**, 2665 (1969).
 - ⁵⁴Experimental studies of the velocity dependence of alkali-metal (²P) + noble-gas intramultiplet cross sections have been reported by several authors; see R. W. Anderson, T. P. Goddard, C. Parravano, and J. Warner, *J. Chem. Phys.* **64**, 4037 (1976); W. D. Phillips, C. L. Glaser, and D. Kleppner, *Phys. Rev. Lett.* **38**, 1018 (1977); J. M. Mestdagh, J. Berlande, J. Cuvelier, P. de Pugo, and A. Binet, *J. Phys. B* **15**, 439 (1982).
 - ⁵⁵R. Düren, E. Hasselbrink, and G. Moritz, *Z. Phys. A* **307**, 1 (1982); and references contained therein.